T-IM/36/2/2/13615

Characteristics and Performance of Minature NBS Passive Hydrogen Masers

F.L. Walls

Reprinted from
IEEE TRANSACTIONS ON INSTRUMENTATION AND MEASUREMENT
Vol. IM-36, No. 2, June 1987

Characteristics and Performance of Miniature NBS Passive Hydrogen Masers

FRED L. WALLS

Abstract—**Recent data on the miniature (30 kg) passive hydrogen masers developed at the National Bureau of Standards (NBS) in cooperation with the Naval Research Laboratory (NRL) indicate a frequency stability of**

$$\sigma_y^2(\tau) \leq (1.5 \times 10^{-12}\,\tau^{-1/2})^2 + (5 \times 10^{-15})^2$$

$$1\ s < \tau < 5 \times 10^5\ s.$$

These masers also have extremely low sensitivity to changes in the external magnetic field or temperature. The sensitivity to barometric pressure and or humidity, although very small, does dominate the residuals in one of the miniature masers for times beyond about a week. Frequency drift is so small as to be hidden in the present measurement precision. The fractional reproducibility under all changes, excluding the storage bulb, appears to be better than 5×10^{-13}. The concepts behind the physics and the electronics that made these advances possible as well as present limitations are explained in some detail.

I. Introduction

THE PASSIVE MASER concept developed at the National Bureau of Standards (NBS) in cooperation with the Naval Research Laboratory (NRL) utilizes the well-known magnetic hyperfine separation in atomic hydrogen shown in Fig. 1 [1], [4]. The concepts developed for this frequency standard make it possible to electronically control the frequency of the microwave cavity to within a few hertz per week. This helps eliminate one of the largest contributions to frequency drift in traditional active (oscillating) hydrogen masers [4]–[9]. The latest version of the NBS passive hydrogen maser is designated miniature passive hydrogen (MPH) maser and is only 26.7 cm high, 66 cm deep, 45.5 cm wide (standard rack width), and weighs 30 Kg. The power requirements are about 55 W at 25°C.

The short-term frequency stability of the first two of the MPH series in a reasonably benign environment is

$$\sigma_y(\tau) = 1.0 \text{ to } 3.0 \times 10^{-12}\,\tau^{-1/2}$$

depending on the flux level. When operating at about $1.5 \times 10^{-12}\,\tau^{-1/2}$, the stability reaches about 4×10^{-15} at two days. Beyond about five days the frequency stability appears to be limited by environmental effects to the mid-10^{-15} ranges. The timekeeping ability is about 0.4 ns at a time prediction interval of one day and about 4 ns at one week.

Manuscript received June 23, 1986. This work was supported in part by the National Bureau of Standards.

The author is with the National Bureau of Standards, Time and Frequency Division, Boulder, CO 80303.

IEEE Log Number 8613615.

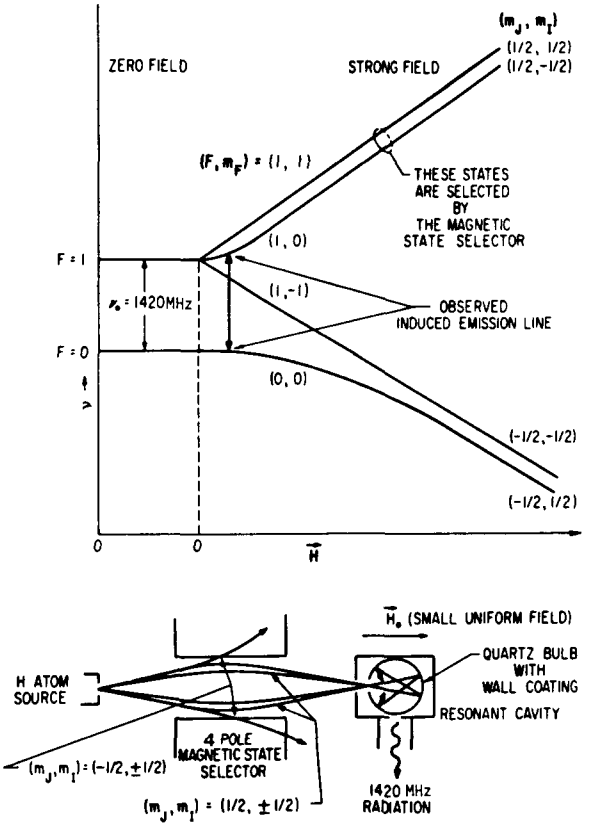

Fig. 1. Hyperfine frequency separation of atomic hydrogen versus magnetic field.

The sensitivity of the output frequency to changes in the external temperature is of order 3×10^{-15}/°C near room temperature. The sensitivity to changes in the external magnetic field is about 9×10^{-15} for $\pm 5 \times 10^{-5}$T (0.5 G). These are so low as to generally not be noticeable in the benign laboratory environment. The one unit operating at the Naval Research Laboratory (NRL) does show a small effect due to the passage of major storms with a peak excursion of order 1×10^{-14} in frequency.

The MPH series has several unique concepts in both the physics package and the electronics which make this performance in such a small size possible. These are described and, where possible, the present limitations are indicated.

II. MPH Discharge and Beam Optics

Fig. 2 shows the general layout of the physics package for the MPH series. The molecular hydrogen storage me-

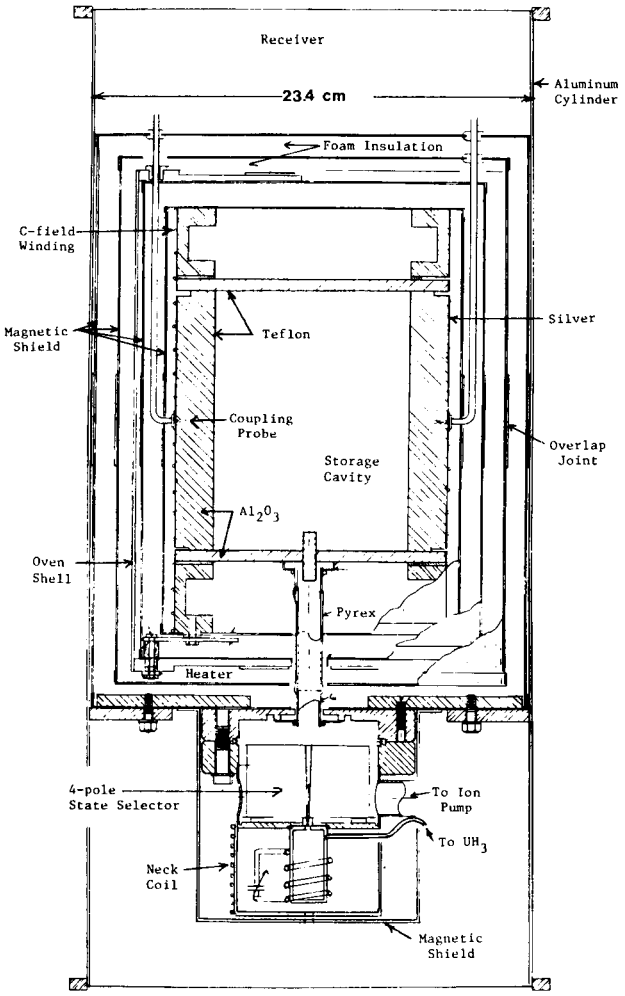

Fig. 2. Sketch of the physics package of the miniature NBS passive hydrogen maser series MPH.

dium for the discharge is uranium hydride (UH_3). The pressure of H_2 over UH_3 is about 1.3×10^{-4} Pa (10^{-6} torr) at 25°C and about 17 Pa (0.13 torr) at 125°C. By regulating the temperature one can adjust the pressure so that the size of the hydrogen signal is kept constant. UH_3 has the additional benefit of being self-cleaning in that it preferentially removes contaminates such as O_2 and N_2 from the discharge bulb. Depleted uranium is only infinitessimally radioactive and easily handled using routine procedures.

The present discharge bulb and oscillator grew out of the work of Persson [11]. The bulb is only 19 mm in diameter and 42 mm long. This geometry minimizes the power required to drive the discharge. Some slight discoloring of the first bulbs was noticed after 18 months with the first discharge excitation coil, which had an RF ground near the exit hole. The new arrangement is more symmetric, with the RF ground at both ends of the bulb, and produces a more uniform glow within the bulb. Even using an old discolored bulb, the required excitation power is only increased by 10 percent as compared to a new bulb and the spectrum of the emitted light is also excellent. The new discharge oscillator operates at about 86 MHz and consumes between 2.5 and 3 W · dc. Increasing the discharge power by a factor of three increases the atomic hydrogen hyperfine transition signal by less than 10 percent. This indicates that the hydrogen is nearly fully dissociated in the center of the discharge bulb. There are not sufficient data to indicate the bulb lifetime with this new arrangement.

The state selector is a quadrupole magnet of length 3.8 cm with a bore tapering from 0.5 to 1.9 mm at the output end. The drivers are samarium–cobalt magnets producing about 0.9 T at the soft-iron pole tips. This provides very efficient defocussing of the two lower hyperfine states shown in Fig. 1 and makes the very short beam optics possible. A weak guiding magnetic field of about 3×10^{-4} T is imposed along the beam path from the state selector to the entrance to the primary magnetic shields. There is also a single magnetic shield around the entire beam optics and discharge region. As explained later in the discussion of systematic effects, this substantially reduces the sensitivity of the output frequency to changes in the external magnetic field by reducing the induced changes in the state population [9].

The vacuum system is pumped by a single 5-l/s ion pump. The estimated pump lifetime at the present flux is of order three years. Since none has failed, even after two years of service, it is not possible to give an accurate lifetime. Sorption pumping would be a good alternative to extend the lifetime beyond ten years. This would also reduce the size (primarily length) somewhat. Note that the microwave cavity is also the storage volume and the vacuum enclosure so that no external vacuum system is necessary. This greatly reduces the surface area and volume that is pumped.

The magnetic shields around the microwave cavity are 0.63 mm thick and are separated by 12 mm. The shields join in the center with an overlapping flange about 51 mm wide. This permits the ends to be spotwelded in place and annealed. This arrangement is very robust and has not shown any significant degradation in the shielding factor of about 200 000 after dozens of assembly–disassembly cycles.

The oven is a single shell of 1.6-mm-thick aluminum with ends of average thickness of about 4.5 mm. It is situated outside the two innermost magnetic shields. This arrangement provides considerable shielding from any stray magnetic fields created by the four power transistors, which are mounted on copper heat sinks and are used to provide the necessary thermal control. The cavity probes are heat sunk to one end of the oven. Thermistors on each end of the oven are used to sense the temperature of the oven. The electronic cavity correction signal is also used to make a small adjustment in the temperature of the oven by introducing a bias into the thermistor bridge. Another thermistor is used to sense the outside case temperature and make a very small change in the oven temperature. This multiple-layered sensor approach holds the cavity to much better than 100 Hz or 1 mK over months. Even better results could be achieved by coupling the cav-

ity more tightly to the oven. Thermal gradients are highly attenuated by the alumina cavity described below.

The storage cavity for both the earlier SPHM NBS passive masers [2] and the new MPH series uses a right circular cylinder of 14.5-cm OD made from low-loss AL_2O_3 ceramic with a 10.5-cm-diameter bore down the central axis. The length is 13.6 cm. The ends are capped with AL_2O_3 plates. The outside of the cylinder and the inside of the end caps are coated with several layers of silver paint, yielding unloaded Q factors between 5500 and 6700. The closed central bore is coated with FEP 120 Teflon.[1] Thus, this dielectrically loaded cavity serves as the microwave cavity, the vacuum chamber, and the storage volume. The integral nature of this design makes it very rugged. An additional feature is that the 2-cm-thick walls of the cavity provide excellent thermal conductivity, thereby minimizing temperature gradients along the storage volume. The microwave coupling loops are located opposite one another in the midplane of the cavity. This reduces any possible residual first-order Doppler effect to less than 10^{-14}, since the effective velocity of the atoms is perpendicular to the energy flow of the probing radiation [1]. This effect could exceed 10^{-13} in small masers without this provision.

III. Hydrogen and Cavity Servo Systems

In the approach developed at NBS, both the output oscillator and the microwave cavity are locked to the hydrogen resonance using the scheme illustrated in Fig. 3 [4]–[14]. A local oscillator signal ultimately synthesized from 5 MHz is phase modulated at two frequencies, f_1 and f_2, before being introduced into the microwave cavity containing the state-selected hydrogen atoms. The transmitted signal is envelope detected and processed in two synchronous detectors, one referenced to the modulation frequency f_1, and the other to f_2. f_1 nominally corresponds to the half-linewidth of the microwave cavity and f_2 nominally corresponds to the half-linewidth of the hydrogen resonance. The output of the f_1 synchronous detector is used to correct the frequency of the microwave cavity with a time constant of about 10 s. As explained earlier, this signal is also used to correct the temperature of the oven with a time constant of about 1 h. The output of the f_2 synchronous detector is used to steer the probe frequency to the center of the hydrogen line with a time constant of 1 or 2 s. Contrary to many schemes, f_2 need not be confined to values less than the half-linewidth of the hydrogen resonance. This is possible since the cavity transmits the sidebands at f_2 even if they lie outside the bandwidth of the atomic resonance as long as they lie within the bandwidth of the cavity. Fig. 4 shows the actual response of the f_2 synchronous detectors as a function of tuning the frequency of the probe oscillator. Note that the dc error

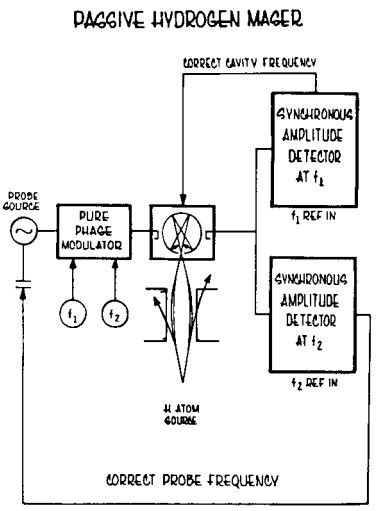

Fig. 3. Sketch of the technique used to lock both the local probe oscillator and the microwave cavity to the hydrogen hyperfine resonance.

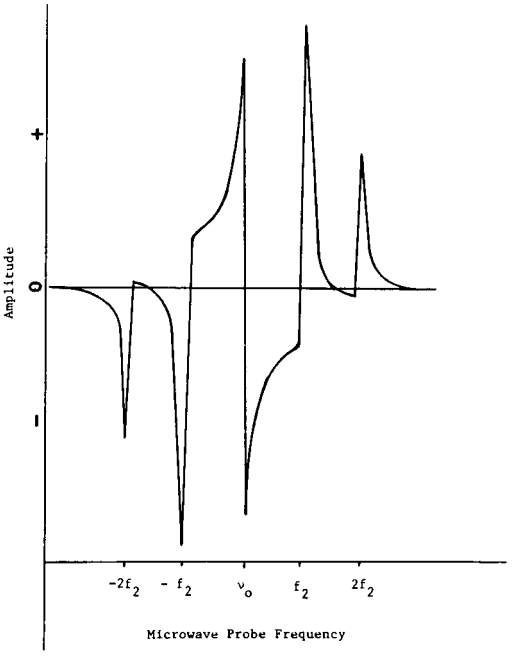

Fig. 4. Output of the f_2 synchronous detector vesus the frequency of the microwave probe.

signal has the proper sign and a significant value for the local oscillator tuned anywhere from $(\nu_0 - f_2)$ to $(\nu + f_2)$. In this example f_2 is about 25 times the half-linewidth of the atomic resonance. This scheme greatly expands the capture range and speeds up the locking of the probe oscillator to the atomic resonance. One of the attractive features of the passive hydrogen maser approach as compared to traditional active hydrogen masers is the ability to lock the frequency of the microwave cavity to the hydrogen line without the need for an external high-stability frequency reference. Several other schemes have recently been introduced for controlling cavity frequencies of hydrogen masers [5]–[8]. Active stabilization of the cavity frequency eliminates, in principle, the largest source of frequency drift seen in traditional active hydrogen ma-

[1]Certain commercial materials are identified in this paper in order to adequately specify the experimental procedure. Such identification does not imply recommendation or endorsement by the National Bureau of Standards, nor does it imply that the materials or equipment identified are necessarily the best available for the purpose.

TABLE I
MPH MASER FREQUENCY PERTURBATIONS

Effect	$\Delta\nu/\nu_0$	− Value	Estimated stability in
2nd Order Doppler	$-1.38 \times 10^{-13}/K$	-4.3×10^{-11}	1.4×10^{-15}
Cavity Pulling and Temperature Coefficient	$\frac{Q_c}{Q_H} \frac{\nu_c-\nu_0}{\nu_0}$	$<2\ 10^{-13}$	$3 \times 10^{-15}/K$
Wall Shift	$\frac{-K \text{ Area}}{\nu_0 \text{ Volume}} [1-\alpha(T-313)]$	-2×10^{-11}	$\leq 2 \times 10^{-13}/y$
Spin Exchange	$\frac{\lambda n_a V_r}{8\pi\nu_0} (\rho_{1,0} - \rho_{0,0})$	$1\text{-}3 \times 10^{-13}$	10^{-15}
Spin Exchange Interruption	$\frac{e_H n_a V_r \sigma}{2\pi\nu_0}$	Included above for passive masers	
Internal Magnetic Field	$2.75 \times 10^{11} \frac{H^2}{\nu_0} (T)^2$	7×10^{-14}	$<2 \times 10^{-15}$
External Magnetic Field Changes		$+ 9 \times 10^{-15}$ for $\pm 5 \times 10^{-5}$ T (±0.5 G)	10^{-15}
Magnetic Field Inhomogeneity Shift	$[K'(\rho_{1,1} - \rho_{1,-1})]$ $\left\langle \frac{H_r^{rf}}{H_Z^{rf}} H_r^{dc} \right\rangle_{bulb}$	$1\text{-}3 \times 10^{-13}$	10^{-15}
Microwave Power		4×10^{-14}/dB	10^{-15}
Phase Modulator Drive		4×10^{-14}/dB	10^{-15}

sers. Servo offsets in the NBS approach are generally of the form

$$\Delta W = K_1\gamma^2 - -\frac{1}{2}M_{2s}\phi - \frac{1}{2}M_{2c} + A_m\frac{\gamma^2}{B} + 2K_{dc}\frac{\gamma^2}{B}$$

where K_1 is the background slope, γ is the angular half-width of the resonance, M_{2c} and M_{2s} are the "in-phase" and "out-of-phase" components of second harmonic distortion in the phase modulation, ϕ is the phase angle between the reference signal and the error signal, A_m is the fractional coefficient of amplitude modulation on the microwave signal which is in phase with the phase modulation, and K_{dc} is the dc offset in the synchronous detector [14]. We have investigated these effects by using the techniques outlined in [14]; these primarily consist of measuring the output frequency while changing the ac gain, modulation width, and ϕ, as well as direct measurements of the residual amplitude modulation at f_1 and f_2 on the microwave probe signal. This exercise shows that there is a frequency offset in the cavity loop which causes an offset in the output frequency of order $1\text{-}2 \times 10^{-13}$. This error appears to be primarily due to the second harmonic distortion in the phase modulator. Harmonic distortion in the synchronous detector is much less important due to the use of a second harmonic notch in the ac amplifier preceding it. The offset due to the cavity servo loop is very stable and is reproduced to within $1\text{-}2 \times 10^{-13}$ for replacement and or retuning of any or all components except for the cavity.

IV. Systematic Effects

Systematic effects which can perturb the output frequency of the maser are listed in Table I along with the expected effect on stability. First-order Doppler effects are extremely small for these devices due to the long storage times and the positioning of the coupling loops discussed above [1].

Hydrogen atoms rapidly thermalize on the wall of the storage cavity. Therefore, changes in the second-order Doppler effects are due to changes in the cavity temperature. The cavity has a temperature coefficient of about 80 kHz/K. The cavity servo loop controls the cavity frequency to within 1 Hz over days and to at least 1 kHz over its functional lifetime. The cavity temperature is therefore bounded by approximately 10 mK, leading to a limit of less than 1.4×10^{-15} for changes in the second-order Doppler effect unless the microwave cavity is changed.

Calculations by Audoin *et al.* [15] and our experimental measurements show that the cavity pulling is given by the expression in Table I, where ν_c is the cavity frequency, ν_0 is the unperturbed hydrogen frequency, Q_c is the quality factor of the cavity, and Q_H is the quality factor of the hydrogen line. Errors in the cavity-tuning servo lead to a measured temperature coefficient of about $1.5 \times 10^{-14}/°C$ unless the case temperature is used to compensate the oven temperature. With this layered thermal sensor approach, the temperature coefficient can be reduced to $3 \times 10^{-15}/°C$ or lower for at least $\pm 4°C$. The comparison of MPH 21 to N1, a new cavity-controlled active maser at NRL, shows a change of 1.5×10^{-14} whenever a large storm comes through the area. It is possible that this is actually a residual temperature effect caused by the change in the air thermal conductivity changing the thermal gradients.

The wall shift has been a topic of considerable controversy over the years [16]–[18]. The notation in Table I is from [16]. The offset is fairly large in masers with small storage volumes. Since we see no frequency drift to within the noise of our measurements of approximately 5×10^{-16}/day on two different models of passive masers, we conclude that the change in the wall shift is probably less than 2×10^{-13}/year. This is quite consistent with a 45-day measurement at Jet Propulsion Laboratories (JPL) simultaneously made on active masers and one of the earlier NBS passive masers, where the frequency could be retraced to within 2×10^{-14} between the various masers after cavity tuning on the active masers. On the other hand, several authors report changes in output frequency which they attribute to changes in the wall shift [19]–[21]. The magnetic field inhomogeneity shift (discussed below) may play a role in some of these measurements [9].

The spin exchange frequency shift given by the expression in Table I is proportional to the total hydrogen density n_a and to the population difference between the (1, 0) state and the (0, 0) state which depends on the microwave power [1], [12]. The experimentally measured frequency shift is $1\text{–}3 \times 10^{-13}$ depending on the flux level and the microwave excitation level. The resolution in setting the hydrogen signal level from the detected $2f_2$ signal out of the receiver relative to the carrier is about 1 percent in several seconds. This approach removes the effect of amplifier gain changes and, to first-order, changes in the microwave excitation level. There is a small error (-10 percent) versus changes in the excitation level due to saturation effects. One could also offset the sidebands used to modulate the probe signal for the cavity lock loop, however, this would significantly complicate the cavity servo system [8]. There is also a small shift of about 4×10^{-4} of the spin exchange broadening or about 10^{-13} due to the interruption of the hyperfine frequency during a spin exchange collision [12]. This effect is included in our measurement of the spin exchange shift but needs to be independently calculated for spin exchange tuned masers.

The sensitivity to changes in the magnetic field (see Table I) is quite small due to the large shielding factor (200 000) of the four magnetic shields and the relatively low operating field of about 265 Hz for the Zeeman frequency f_z. With the shielding factor of 200 000, the expected fractional frequency shift for a change in the external magnetic field of $\pm 5 \times 10^{-5}$ T (0.5 G) is $\pm 2 \times 10^{-15}$. The measured value is $+9 \times 10^{-15}$ for either + or -5×10^{-5} T, indicating a nominal quadratic dependence on external magnetic field. This performance is about a factor of 30 better than that obtained without the guiding field and the magnetic shield around the beam path. This result is clearly not just due to the change of the magnetic field in the microwave cavity. The most likely explanation is that it is due to the magnetic field inhomogeneity shift (Crampton effect) coupled with a change in the mixing of states along the beam path from the state selector to the entrance to the magnetic shield package [12]. Fig. 5 shows the output frequency of MPH 14 versus the square of the Zeeman frequency for several configurations of the magnetic field and neck coil. Note that when there is nominally no field reversal in magnetic field along the beam path, the slope of the output frequency with magnetic field has the theoretical slope but not necessarily the correct intercept for zero magnetic field due to the Crampton effect [12]. After the results shown in curve *A* were obtained, the maser was degaussed again ending with even smaller ac currents. A neck coil was used to produce an axial magnetic field along the beam path of about 3×10^{-4} T aligned with the internal magnetic field. The output frequency versus the Zeeman frequency then performed as shown in curve *B*. In both cases the (1, −1) state population was about 20 percent of the (1, 1) state. The ratio of the populations of the (1, 1) state to the (1, −1) state was measured by comparing the relative amplitudes of the signal derived by driving the maser at $(\nu_0 + f_z)$ to that obtained at $(\nu_0 - f_z)$. Curve *C* was obtained by nominally equalizing the populations of the upper Zeeman sublevels by careful adjustment of the neck coil to reduce the magnetic field along the beam path to approximately zero (see Fig. 1). Present theory predicts that the value of the output frequency is unaffected by the Crampton effect when the populations of (1, 1) and (1, −1) are equal. Curve *D* was obtained by inverting the state populations coming out of the state selector. This was accomplished by using the neck coil to produce an axial magnetic field of about 3×10^{-4} T opposed to the internal magnetic field. The slope is not very close to the theoretical one for curves *C* and *D*, presumably due to the fact that changing the internal magnetic field also changes the abruptness of the transition in magnetic field direction along the beam path and therefore changes slightly the state populations. This changes the value of the Crampton effect. It is reassuring that the value of the output frequency obtained by extrapolating curves *B* and *D* to zero magnetic field is symmetrically placed relative to curve *C* to within 3×10^{-14}. When there is a field reversal along the beam path the slope is often different from theoretical and the intercept may differ from the nonreversed value by several parts in 10^{+13}. By very careful

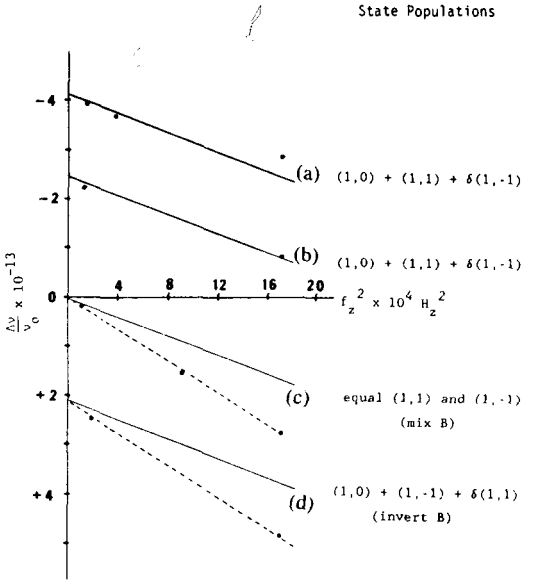

Fig. 5. Fractional change in the output frequency versus the square of the Zeeman frequency. (a) Coarse degauss of MPH 14 for the standard alignment of the internal magnetic field and the state selector. δ is of the order 20 percent. (b) Careful degauss of MPH 14. The residual magnetic fields are less than 20×10^{-11} T (20 μG). (c) Adjustment of neck coil to approximately equalize the (1, 1) and (1, −1) states. (d) Adjustment of neck coil to invert the populations shown in curve *B*. The solid lines show the expected slope from the Breit-Rabi theory [1].

adjustment of the internal *c*-field, and the guiding field along the beam path, this effect can be reduced. The other method, which reduces the shift and also reduces the spin exchange shift, is to use two state selectors separated by a region in which the state populations are inverted from (1, 1) and (1, 0) to (1, −1) and (1, 0). After passage through the second state selector the beam ideally contains only the (1, 0) state [22], [23]. Unfortunately, this lengthens the beam path and probably is not practical in very small units. The magnetic field inhomogeneity shift very likely was a problem in the early measurements of the unperturbed value of the hydrogen hyperfine frequency where the storage bulb was changed many times [8], [17]-[19]. It may also have been a problem in some of the measurements of wall shift versus time.

There is a small dependence of output frequency on the excitation power via the change in the spin exchange shift and the offsets in the servo systems. This effect is measured to be approximately 4×10^{-14}/dB change in the microwave power. Likewise, there is a very small dependence on the modulation width in the cavity servo of 4×10^{-14}/dB [14].

Several passive masers of both the earlier SPHM version and the present MPH variety, which have been opened to air for servicing and repumped, have recovered frequency to within 2×10^{-13}. MPH 21 was sent by commercial air to Washington, DC, and recovered frequency to within 1×10^{-13} without being degaussed.

V. Frequency Stability and Timekeeping Results

Frequency stability and the timekeeping ability of MPH 14 and MPH 21 have been analyzed using a wide variety of references. Fig. 6 shows a composite of some of these measurements. The frequency stability in short term for both masers is typically given by

$$\sigma_y(\tau) = 1.5 \times 10^{-12}\, \tau^{-1/2} \qquad 1\ s < \tau < 10^5\ s.$$

At somewhat higher flux levels we have observed stabilities of

$$\sigma_y(\tau) = 1.0 \times 10^{-12}\, \tau^{-1/2}, \qquad 1\ s < \tau < 100\ s.$$

This is in good agreement with the theoretical calculations of Audoin and colleagues for this cavity [12]. Improvements of up to a factor of 10 appear possible by using microwave cavities with higher intrinsic Q factors [4], [15]. The frequency stability beyond a day begins to depend on the environment. In an environment with temperature variations below 0.5 K and no magnetic disturbances in excess of 10^{-5} T (0.1 G) the stability continues to improve until reaching approximately 4×10^{-15} at two days. Measurements versus an active maser with electronic cavity tuning [6], [24] at NRL (Fig. 6) yield extraordinary performance for both clocks out to five days. There is a small perturbation in the phase comparison between the two in Fig. 7(c) which appears to be primarily attributable to MPH 21 and correlates with the passage of a large storm system with barometric pressure changes of approximately 10 percent. These data are generally consistent with those shown in Fig. 6 for MPH 14 compared against the NBS time scale which is primarily composed of cesium clocks. MPH 14 was about 24 percent of the time scale over the 50-day period. The white frequency level data of MPH 14 versus the NBS time scale is clearly dominated by the cesium clocks from 2 h out to at least several days. At ten days the stability for the MPH 14 versus the time scale is similar to that measured at NRL against MPH 21 at five days. A search for frequency drift between the scale and MPH 14 over this data yields

$$\Delta\nu/\nu = 2 \pm 5 \times 10^{-16}/\text{day}.$$

The NRL data yielded a drift between the two masers of about 9×10^{-16}/day, however, there are not yet enough data to confirm that drift is a good model. Fig. 7 shows time dispersion data for both MPH 14 and MPH 21. Based on the data above for both MPH 14 and MPH 21, the time dispersion of this style of miniature maser varies from about 0.4 ns for a time prediction interval of one day to about 4 ns at an interval of seven days.

VI. Failures and Other Problems

In the process of working on passive masers over the past several years we have observed a number of frequency shifts and changes. The number one trouble has been power outages and power surges due to severe lightning activity. The problems that have appeared due to this are failures in operational amplifiers presumably from high voltage-current pulses, and the "gaussing up" of magnetic shields due to being located too near the ac bus lines, which changes the Crampton effect.

On several occasions we have observed drift in the out-

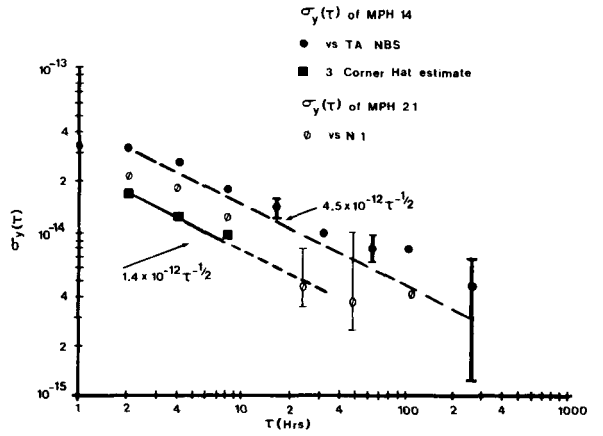

Fig. 6. Fractional frequency stabilites of MPH 14 versus the NBS atomic time scale primarily composed of cesium standards. (Also shown is the stability of MPH 21 versus N1, an experimental active maser at NRL. No drift has been subtracted from any of the data and no adjustments have been made for instability of the reference except in the three-corner hat estimate.)

put frequency. Usually this proved to be due to insufficient degaussing after being moved or after being exposed to a large external magnetic field such as produced by an ion pump magnet or being located too close to a power line that suffered a large current surge. The drift disappears after a high-current degauss, which for us involves a single loop through the innermost shield with about 200 A at 60 Hz followed by a very low-current degauss. One case where this was not true was traced to leakage on the board into the integrator for the cavity servo system. Another was traced to a failure in one of the FET's used in the synchronous detector for the cavity servo. On several occasions frequency changes of 1–2 parts in 10^{-14} have occurred between the maser and the reference which were never identified.

The addition of the shield and guiding field along the beam paths has reduced the sensitivity to magnetic effects and a line conditioner has helped with the line surges.

VII. Conclusion

It has been experimentally demonstrated that the MPH design of passive hydrogen maser yields a relatively small clock capable of excellent timekeeping performance. The reproducibility of the output frequency is better than 5×10^{-13} for substitution of all the electronics except the microwave cavity.

The frequency stability in a benign environment is given by

$$\sigma_y^2(\tau) = (1.5 \times 10^{-12}\,\tau^{-1/2})^2 + (5 \times 10^{-15})^2,$$
$$1\,s < \tau < 5 \times 10^5\,s.$$

The timekeeping uncertainty is approximately 0.4 ns per day and 4 ns per week. Frequency drift is at most a few parts in 10^{-16}/day and is very difficult to resolve from measurement noise and or changes in available frequency references. The sensitivity to changes in the ambient temperature have been reduced to approximately 3×10^{-15}/K and the sensitivity to changes in the external magnetic field to $9 \times 10^{-15}/\pm 5 \times 10^{-5}$ T. There is a small sensitivity to humidity or barometric pressure.

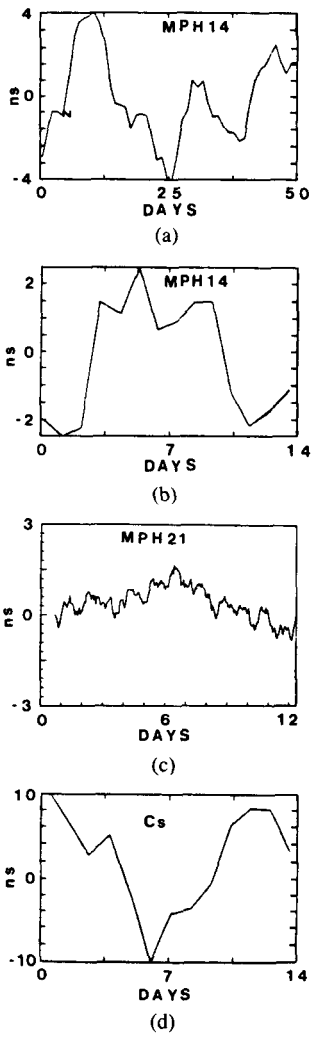

Fig. 7. (a) and (b) The time of MPH 14 versus the NBS time scale. (c) The time of MPH 21 versus N1. (d) Comparison of the time of one of the best NBS commercial cesium standards.

Acknowledgment

The author is very grateful to the Naval Research Laboratory (NRL) for long-term support for the passive hydrogen program and especially to Dr. J. White and A. Gifford of NRL for helping in the early troubleshooting and analyzing much of the data on MPH 21. The author is also very grateful to my colleagues at the National Bureau of Standards (NBS) for many fruitful discussions, and in particular to D. A. Allan who has helped in much of the analysis of the various passive masers versus the NBS time scale, and provided encouragement; to D. A. Howe who originally designed the dielectrically loaded cavity, the magnetic shield package, and aided in the design of the electronics; to K. B. Persson who has assembled the recent cavities and developed the theory that led to the low-power hydrogen discharge system; to C. Manny who designed the precision frequency multipliers, to D.

Hilliard who with A. C. Clements and C. M. Felton[2] attended to many of the practical details of these new masers; and to M. A. Dials, L. Wert, T. Smith, and S. R. Stein who provided the small offset frequency synthesizer, receiver, and discharge oscillator; and to L. L. Lewis who originally suggested using the case temperature as an additional feedback to the oven compensation.[3]

References

[1] D. Kleppner, H. M. Goldenberg, and N. F. Ramsey, "Properties of the hydrogen maser," *Appl. Opt.*, vol. 1, pp. 55-60, 1962.

[2] D. Kleppner, H. M. Goldenberg, and N. F. Ramsey, "The theory of the hydrogen maser," *Phys. Rev.*, vol. 126, pp. 603-615, 1962.

[3] D. Kleppner *et al.*, "Hydrogen maser principles and techniques," *J. Phys. Rev. A*, vol. 138, pp. 972-983, 1965.

[4] F. L. Walls and D. A. Howe, "Timekeeping potentials using passive hydrogen masers," *J. de Physique*, Colloque C8, vol. 42, C8-151-158, 1981.

[5] Private communication, Smithsonian Astrophysical Observatory, Cambridge, MA 1985.

[6] G. A. Gifford, J. D. White, and H. E. Peters, "Hydrogen maser research and development at Sigma Tau standards and tests of Sigma Tau masers at the Naval Research Laboratory," in *Proc. 17th Precise Time, Time Interval (PTTI)* (Washington, DC), 1985, pp. 105-128.

[7] G. J. Dick and T. K. Tucker, "Fast Autotuning of a hydrogen maser by cavity Q modulation," in *Proc. 17th Precise Time, Time Interval (PTTI)* (Washington, DC), 1985, pp. 129-144.

[8] H. T. M. Wang, "Characteristics of oscillating compact hydrogen masers," in *Proc. 36th Annu. Symp. Freq. Control* (Springfield, VA), 1982, pp. 249-254.

[9] F. L. Walls and K. B. Persson, "A miniatured passive hydrogen maser," in *Proc. 38th Annu. Symp. Freq. Control* (Piscataway, NJ), 1984, pp. 416-419.

[10] F. H. Spedding, A. S. Newton, J. C. Warf, O. Johnson, R. W. Nottorf, I. B. Johns, and A. H. Daare, "Uranium hydride 1—Preparation composition, and physical properties," *Nucleonics*, pp. 4-15, 1949.

[11] K. B. Persson and F. L. Walls, "Investigation of Hydrogen Sources for Masers, Nat. Bur. Stand., NBS Tech Note, to be published.

[12] "Density-dependent shifts to hydrogen maser standards," S. Crampton and H. Wang, in *Proc. 28th Freq. Control Symp.*, 1974, pp. 355-361.

[13] F. L. Walls, "Frequency Stabilization Utilizing Multiple Modulation," U.S. Patent 4 122 408 assigned to the U.S. Dept. of Commerce.

[14] F. L. Walls, "Errors in servosystems using sinusoidal frequency (phase) modulation," in *Proc. 39th Ann. Symp. Freq. Contr.* (Piscataway, NJ), 1986, pp. 91-95.

[15] P. Lesage, C. Audoin, and M. Tetu, in *Proc. 33rd Annu. Symp. Freq. Contr.*, 1979; also C. Audoin, J. Viennet, and P. Lesage, "Hydrogen maser: Active of passive?" *J. de Physique*, Colloque C8, vol. 42, C8-159-170, 1981.

[16] J. Vanier, R. Larouche, and C. Audoin, "The hydrogen maser wall-shift problem," in *Proc. 29th Annu. Symp. Freq. Contr.*, 1975, pp. 371-382.

[17] H. Hellwig, R. F. C. Vessot, M. W. Levine, P. W. Zitzewitz, D. W. Allan, and D. J. Glaze, "Measurement of the unperturbed hydrogen hyperfine transition frequency," *IEEE Trans. Instrum. Meas.*, vol. IM-19, 1970.

[18] P. Petit, M. Desainfuscien, and C. Audoin, "Temperature dependence of the hydrogen maser wall shift in the temperature range 295-395 K," *Metrologia*, vol. 16, pp. 7-14, 1980.

[19] D. Morris, "Time-dependent frequency shifts in the hydrogen maser," *IEEE Trans. Instrum. Meas.*, vol. IM-27, pp. 339-343, 1978.

[20] L. U. Hibbard, "Development of the CSIRO hydrogen maser," *J. Elec. Electron. Eng. Aust.*, vol. 1, pp. 243-250, 1981.

[21] B. A. Gaigerov, G. A. Elkin, and N. D. Zhestkova, "Fundamental directions of hydrogen generator development," *Izmer. Tekhn.*, no. 12, pp. 38-40, Dec. 1983.

[22] H. E. Peters, "Magnetic state selection in atomic frequency and time standards," in *Proc. 13th Annu. Precise Time, Time Interval Applications, Planning Meeting* (Washington, DC), 1981, pp. 645-666.

[23] R. F. C. Vessot, private communication, Smithsonian Astrophysical Observatory, Cambridge, MA, 1985.

[24] H. E. Peters and P. J. Washburn, "Atomic hydrogen maser active oscillator and bulb design optimization," in *Proc. 16th Annu. Precise Time, Time Interval (PTTI) Applications and Planning Meeting* (Washington, DC), 1984, pp. 313-338.

[2]Outside contractor Felton Electronic Design, Boulder, CO.

[3]EFRATOM Division Ball Corporation, Broomfield, CO, working through the Industrial Research Associateship Program.